Geophysical Research Letters®

Key Points:

- Extracted first principal component, highly correlated with high cloud fraction, isolating meteorological effects on clouds
- Dust facilitates ice crystal formation and precipitation, catalyzing cloud lifecycle and ultimately modifying radiative effects
- Increased dust accelerates high cloud lifecycle, causing more extreme weather and mitigating climate warming

Correspondence to:

J. Huang,
hjp@lzu.edu.cn

Author Contributions:

Conceptualization: Jinming Ge, Wenxue Li, Jianping Huang, Xiaoyu Hu
Data curation: Jing Su, Khan Alam, Xiaoyu Hu
Funding acquisition: Jianping Huang
Investigation: Khan Alam, Zeen Zhu
Methodology: Jinming Ge, Wenxue Li, Qinyu Mu, Qingyun Zhao, Yongkun Xie, Zeen Zhu, Xiaoyu Hu
Project administration: Jianping Huang
Resources: Khan Alam, Zeen Zhu
Software: Wenxue Li, Qinyu Mu, Yongkun Xie
Supervision: Jianping Huang, Qingyun Zhao, Khan Alam
Validation: Wenxue Li, Qinyu Mu, Qinghao Li

Dust Accelerates the Life Cycle of High Clouds Unveiled Through Strongly-Constrained Meteorology

Jinming Ge[1], Wenxue Li[1], Jianping Huang[1], Qinyu Mu[1], Qinghao Li[1], Qingyun Zhao[1], Jing Su[1], Yongkun Xie[1], Khan Alam[1,2], Zeen Zhu[3], and Xiaoyu Hu[4,5]

[1]Key Laboratory for Semi-Arid Climate Change of the Ministry of Education and School of Atmospheric Sciences, Lanzhou University, Lanzhou, China, [2]Department of Physics, University of Peshawar, Peshawar, Pakistan, [3]Environmental and Climate Sciences Department, Brookhaven National Laboratory, Upton, NY, USA, [4]Chongqing Research Institute of Big Data, Peking University, Chongqing, China, [5]School of Mathematical Sciences, Peking University, Beijing, China

Abstract Dust and high cloud interactions are critical for climate change, primarily due to the dominant roles of high cloud in the greenhouse effect and the continental precipitation. Nonetheless, disentangling the specific impacts of dust from the overlying meteorology influence on high clouds presents great challenges. In this study, we construct a meteorological pattern that successfully reveal the intricate connection between high cloud distribution and atmospheric conditions. Through this strong bounded relationship, we find that dust exhibits notable controls over the facilitation or inhibition of ice particle growth contingent upon the prevailing meteorological fields. More dust can increase precipitation rate and shorten high cloud lifetime particularly under favorable meteorology. These findings underscore the crucial role of dust concentration in mitigating global warming for future climate change.

Plain Language Summary Dust particles in the atmosphere play a crucial role in the formation and dissipation of high clouds, which can significantly impact global climate and weather patterns. By analyzing satellite observations and climate model data, we discovered that dust can either enhance or suppress the growth of ice crystals, depending on the atmospheric conditions. In moist environments with favorable weather, increased dust leads to larger ice crystals and more precipitation, accelerating the life cycle of high clouds. Conversely, in dry conditions with unfavorable weather, excessive dust competes for limited moisture, resulting in smaller ice crystals, although it can still increase rainfall during the dissipation stage of high clouds. As climate change progresses and dust storms become more frequent, the increased presence of dust in the atmosphere may lead to more extreme weather events and potentially mitigate some of the warming effects caused by high clouds. Understanding these complex interactions between dust, high clouds, and weather conditions is essential for improving climate models and predicting future changes in Earth's water cycle and energy balance.

1. Introduction

Dust, as the most abundant atmospheric aerosol in terms of mass, has long been recognized for its crucial roles in modulating Earth's climate (Creamean et al., 2013; Huang et al., 2014, 2019; Kok et al., 2023). Dust particles can serve as ice nucleating particles (INPs), seeding high cloud formations under relatively low humidity and high temperature through heterogeneous freezing (Boose et al., 2016, 2019; Cziczo et al., 2013; Froyd et al., 2022; Hoose & Möhler, 2012; Kuebbeler et al., 2014; Zhao et al., 2019). This procedure, known as the aerosol-cloud interaction (ACI), significantly modifies the microphysical properties of high clouds, such as ice particle size and number concentration, and subsequently the macrophysical features including cloud fraction, height, and lifetime (Andreae & Rosenfeld, 2008; Fan et al., 2016; J. Huang et al., 2014; Seinfeld et al., 2016; Sorooshian et al., 2019; Zhao et al., 2018). High cloud exerts a net warming effect and plays a dominant role on continental precipitation, considering their vast coverage (30%) over Earth's surface, minor changes in high cloud properties induced by dust aerosols can substantially perturb Earth's energy budget and hydrologic cycle (Gasparini et al., 2018; Liou, 1986; Lohmann & Gasparini, 2017; Rosenfeld et al., 2008; Stevens & Feingold, 2009).

Recent investigations indicate a notable rise in dust storm frequency and intensity (Chen et al., 2023; Liu et al., 2021). These particles, when reaching the upper troposphere, can travel long distances and enhance high cloud formation at lower altitudes through heterogeneous nucleation (Ault et al., 2011; Creamean et al., 2013; Uno et al., 2009). This phenomenon has the potential to alter the warming effect of high clouds compared to those

Visualization: Qinyu Mu
Writing – original draft: Jinming Ge
Writing – review & editing: Jinming Ge, Qinyu Mu, Qingyun Zhao, Jing Su, Xiaoyu Hu

formed homogeneously. However, the high cloud lifecycle, determined by the cloud formation and dissipation processes, are strongly controlled by atmospheric dynamical and thermodynamical factors such as temperature, relative humidity, and stability. Decoupling dust-induced impacts on high clouds from meteorological variations remains a formidable challenge. The lack of consensus regarding the magnitude and direction of the impacts of dust on high clouds in previous studies has induced considerable uncertainties in estimating the radiative forcing of dust ACI, posing substantial challenges for future climate projections (J. Huang et al., 2006; Ma et al., 2018; Patel et al., 2019; Rosenfeld et al., 2001).

In this study, we constructed a meteorological pattern that reasonably explains the observed high cloud fraction (HCF) on a global scale. We mainly focus on the Tibetan Plateau (TP) region for its pristine environment and abundance of dust aerosol and high clouds over this elevated topography (J. Huang et al., 2023; Liu et al., 2021; Wu et al., 2015), providing a unique opportunity to investigate the effect of dust aerosol fluctuations on high clouds (Ge et al., 2014; Hu et al., 2020). We employed aerosol, cloud, precipitation, and radiation data from multiple satellites and reanalysis datasets and capitalized on the well-constrained meteorology to quantify the dust effects on micro- and macro-physical properties of high clouds. Dust ACI impacts on precipitation and Earth's radiation budget in the context of global warming are clearly revealed.

2. Data and Methodology

2.1. Observation Data

We analyze aerosol characteristics, cloud properties, and atmospheric conditions using a comprehensive set of satellite observations and reanalysis datasets for an 11 year period form 2010 through 2020. For aerosol properties, we utilize the Multi-angle Imaging Spectrometer (MISR) aerosol product (NASA/LARC/SD/ASDC, 2008) to obtain daily aerosol optical thickness and type at a spatial resolution of $0.5° \times 0.5°$. Additionally, we incorporate hourly dust aerosol optical depth data from the Modern-Era Retrospective Analysis for Research and Applications, Version 2 (MERRA2) (Global Modeling and Assimilation Office, 2015), covering the same period and region, with a resolution of $0.625° \times 0.5°$.

To assess cloud properties, including ice particle radius (Ri), ice water path (IWP), HCF, and high cloud optical depth (COD) at the top of the atmosphere, we employ the Clouds and the Earth's Radiant Energy System (CERES) SYN1deg-Ed4.1 A dataset (NASA/LARC/SD/ASDC, 2017). This dataset integrates observations from both geostationary and polar-orbiting satellites and provides incoming solar radiative fluxes and outgoing longwave radiative fluxes under all-sky and clear-sky conditions at the top of the atmosphere (i.e., F_{SWall}, F_{LWall}). Following the approach of Rajeevan and Srinivasan (2000), we calculate the net cloud radiative forcing as:

$$CRE_{Net} = F_{LWclr} - F_{LWall} + F_{SWclr} - F_{SWall}$$

Meteorological conditions are obtained from the European Center for Medium-Range Weather Forecasts v5 reanalysis (Hersbach et al., 2023), providing hourly data of vertical velocity, horizontal wind speed, temperature, relative humidity, and stability parameters at a spatial resolution of $0.25° \times 0.25°$. For precipitation observations, we use the Global Precipitation Measurement (GPM) 3IMERGHH product (Huffman et al., 2023), offering high-precision, half-hourly measurements at a fine spatial resolution of $0.1° \times 0.1°$. To ensure consistency, all datasets are averaged to daily temporal resolution and interpolated to a $1° \times 1°$ spatial grid using cubic spline interpolation. These carefully selected datasets are well-suited for examining aerosol impacts and cloud dynamics over the specified region and period, offering detailed and accurate measurements crucial for our study.

2.2. PCA and Cloud Susceptibility Calculation

Principal Component Analysis (PCA) (Evan et al., 2016) is employed to transform the high-dimensional meteorological dataset (i.e., vertical velocity, U-component of wind speed, temperature, relative humidity, and stability) into a one-dimensional dataset. To form this dataset, we first reshape the data into a two-dimensional array where each row represents the spatiotemporal distribution of a specific meteorological factor, and each column represents one of the five parameters. We then standardize all five meteorological parameters to have zero mean and unit variance for consistency, eliminating the influence of different units. The direction and magnitude of the variance for these factors are derived by computing the eigenvectors and eigenvalues of the dataset. By sorting eigenvalues and their eigenvectors, we identify principal components. The first principal component (PC1),
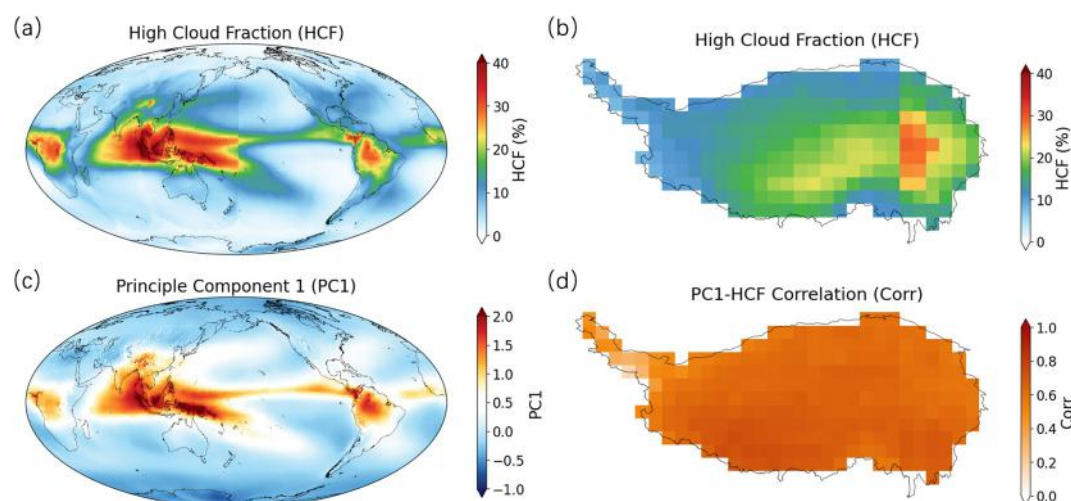
Figure 1. The relationship between PC1 and high cloud fraction. (a) Global high cloud fraction derived from CERES data spanning over 2010–2020. (b) High cloud fraction distribution over the Tibetan plateau. (c) The leading mode of the meteorological conditions derived from the ERA5 reanalysis data during the same period. (d) The correlation coefficient distribution between leading mode of meteorology and high cloud fraction over the TP, all grid points have passed the 99% significance test and hence the correlation coefficients of our total spatial section are significant.

which extracts the maximum variation of the meteorological factors, is selected as our one-dimensional representation. This PC1 corresponds well to the atmospheric conditions under cloudy sky and is confirmed to have a good correlation with high cloud fraction.

To quantify the sensitivity of cloud properties to aerosol loading, we calculate the cloud susceptibility following the approach of Rosenfeld et al. (2019). The susceptibility of a cloud property (*Cld*) to aerosol optical depth (AOD) is defined as the logarithmic derivative: $\partial \ln (Cld) / \partial \ln (AOD)$, where *Cld* can be HCF, IWP, etc. This is well known to represent the relative change in the cloud property for a change in aerosol loadings.

3. Results

3.1. Constraints of Meteorological Conditions on High Cloud

The difficulty in quantifying ACI is distinguishing cloud responses to meteorology from those to aerosol loading changes. We first examine the sensitivity of global HCF to five key high-level meteorological factors (vertical air velocity, horizontal wind, stability, temperature, and relative humidity at 300 hPa), which largely control high cloud formation and dissipation processes. These factors have clear effects on HCF (Figure S1 in Supporting Information S1); however, no single variable fully encapsulates the cloud distribution. Considering the synergistic effects of diverse meteorological factors on clouds and the broader spectrum of meteorological fluctuations in overcast conditions compared to clear sky conditions, we employed PCA to identify the maximum variance direction of these five parameters and consolidated them into a singular variable. The principal component captures the primary pattern of meteorological factors aligned with cloud presence, as evidenced by the partial correlation coefficients in Table S1 in Supporting Information S1.

The left column in Figure 1 shows the HCF from 11 years of CERES data alongside PC1 derived from ERA5 data during the same period. PC1 explains approximately 41% of the meteorological variations, and its spatial structure (Figure 1c) is strikingly similar to the HCF distribution (Figure 1a). Positive PC1 values represent weather conditions that favor cloud formation, while negative PC1 values indicate conditions that promote cloud dissipation (see in Figure S1 in Supporting Information S1). Regions with high HCF and positive PC1 values are concentrated in the intertropical convergence zone and monsoonal regions, notably East and South Asia. Conversely, areas with lower HCF are found in the subtropical subsidence zone and high latitudes, corresponding to negative PC1 values. Figures 1b and 1d show the HCF over the TP region and their correlation to PC1 in each grid. The HCF is highly correlated with PC1, with correlation coefficients greater than 0.7 over most areas of the TP. This consistency strongly suggests that the complex meteorological controls on high clouds can be well
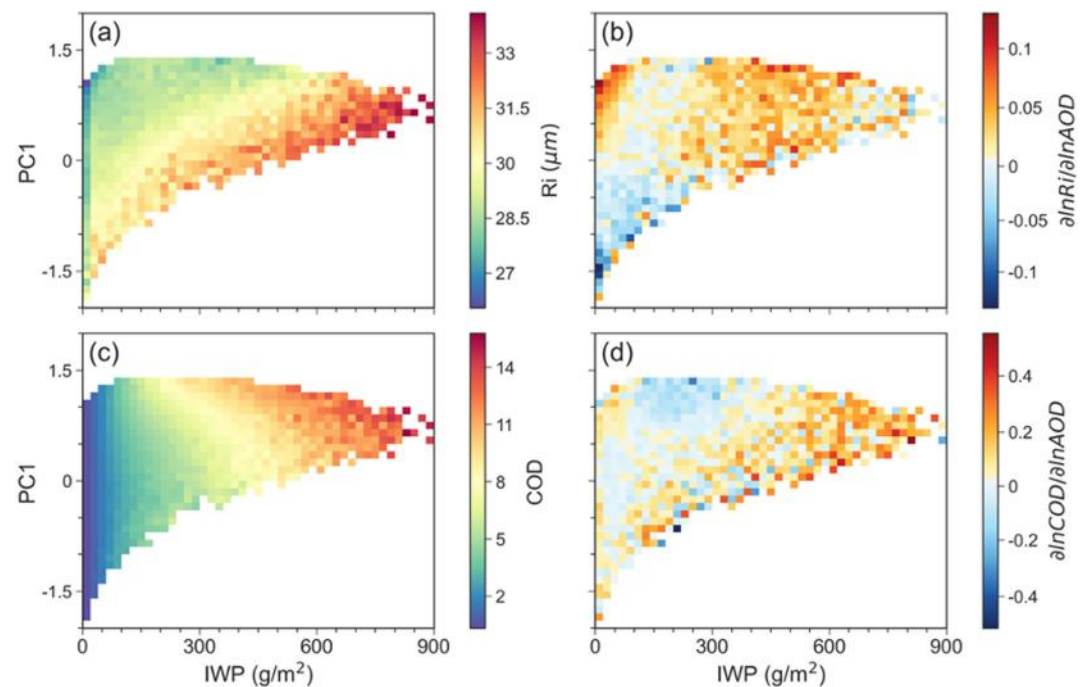
Figure 2. The distributions of high cloud particle effective radius (Ri) and high cloud optical depth (COD), and their susceptibilities to AOD with variations of PC1 and IWP. (a) Ri sorted by the PC1 and IWP; (b) Linear regressions of ln (Ri) against ln (AOD) in each PC1-IWP bin; (c) COD sorted by the PC1 and IWP; (d) Linear regressions of ln (COD) against ln (AOD) in each PC1-IWP bin.

represented by this PCA-compressed variable. Consequently, PC1 effectively constrains meteorological influences on high cloud dynamics in the horizontal domain.

3.2. Dust Effects on High Cloud Microphysical Properties

We divide the PC1 value, mostly falling within −1.5 to 1.5, into 30 bins with a 0.1 interval to represent similar meteorological conditions in each bin. We also use IWP, the integral of the ice water content in the atmospheric column, as another constraint for water vapor supply and cloud vertical development. We then combine PC1 and IWP to indicate the formation (conducive meteorology for clouds with small IWP), development (conducive meteorology for clouds with large IWP), and dissipation (unfavorable meteorology) stages of clouds and investigate the relationship between high cloud microphysical properties and aerosol optical depth (AOD).

Figure 2 shows the variations of Ri, COD, and their susceptibility to the perturbation of dust AOD composited with respect to PC1 and IWP. In Figure 2a, Ri generally grows with an increase of IWP and has a relatively larger value under unfavorable meteorological conditions (smaller PC1) than under favorable meteorology (larger positive) for a given IWP. The susceptibility of Ri to dust loading shown in Figure 2b is more positively sensitive to dust AOD in two areas. One is located at the bins with large positive PC1 (>0.6) and very low IWP (<80 g m^{-2}), corresponding to the beginning of the high cloud formation stage with newly formed ice particles. The other is at the bins with IWP > 300 g m^{-2}. These bins mostly locate at the southern part of the TP where water vapor is sufficient to supply cloud development (Figures S2b-S2d in Supporting Information S1).

In these regions, increased dust AOD enhances the heterogeneous nucleation process and increases the ice-phased particle number concentration. Ice crystals continue to grow even under unfavorable meteorology through microphysical processes such as aggregation and riming, as seen in the positive susceptibility with slightly negative PC1 in Figure 2b. Notably, as meteorological conditions strengthen, the positive susceptibility of high clouds to dust AOD weakens, indicating meteorology increasingly influences high cloud particle growth. While negative bins are present at large negative PC1 with low IWP and high dust occurrence frequency. Under relatively dry environments favoring cloud dissipation, increasing dust INPs results in negative susceptibility of Ri, meaning the presence of small ice particles. This inhibition process can be explained either by the fierce
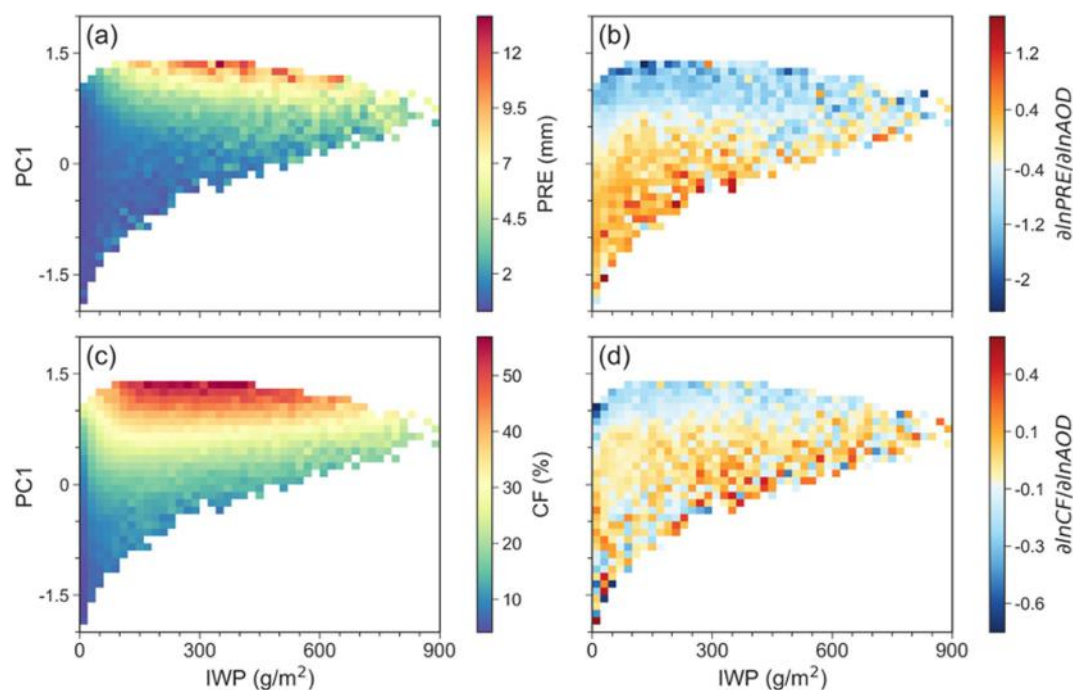
Figure 3. Same as Figure 2 but for (a) Cumulated Precipitation (PRE) sorted by PC1 and IWP; (b) Linear regressions of ln (PRE) against ln (AOD) in each PC1-IWP bin; (c) High cloud fraction (CF) sorted by PC1 and IWP; (d) Linear regressions of ln (CF) against ln (AOD) in each PC1-IWP bin.

competition for the limited water vapor or by the enhancement of ice crystal evaporation at the dissipation stage. This phenomenon is particularly obvious on the northern slope of the TP, where abundant dust aerosol can be vertically transported from the Taklimakan Desert.

COD is derived from the vertical integrations of cloud extinction coefficient, mainly determined by cloud particle size, number concentration and their vertical distribution. Therefore, COD is strongly dependent on IWP in Figure 2c. The susceptibility of COD to AOD is intricate, as shown in Figure 2d. When the atmosphere has adequate water vapor supply (IWP > 500 g m^{-2}), increased dust INPs can lead to larger COD, boosting ice crystal concentration and total extinction cross-section, thereby enlarging HCF and thickness on a macro scale. However, with strong positive and moderately negative PC1 and IWP ranging from 80 to 300 g m^{-2}, COD shows negative sensitivity to dust burden. Those negatively correlated regions between COD and dust are located at the northern and southern edges of TP (Figure S3b in Supporting Information S1). One may note that these areas either correspond to the favorable atmospheric conditions for cloud development and heavy precipitation (shown in Figure 3a), or large positive susceptibility of precipitation under relatively conducive conditions for cloud dissipation (Figure 3b). We may infer that under moderate water vapor supply, dust promotion on high cloud development is less effective than its enhanced sedimentation process that induces a decrease of COD over these regions.

3.3. Dust Effects on Precipitation, High Cloud Fraction and Radiative Forcing

The daily accumulated precipitation strongly correlates with PC1, as depicted in Figure 3a, signifying that the PCA method effectively captures the meteorological influences on precipitation. The response of precipitation to AOD can be categorized into negative and positive regimes, distinguished by a PC1 threshold of around 0.3 (Figure 3b).

In the lower regime, where PC1 values range from negative to weakly positive (<0.3), increasing dust aerosols evidently enhances precipitation (Figure S5 in Supporting Information S1) as more dust INPs promote ice-phase particle formation (Figure 2b), consequently enhancing precipitation initiation. In the upper regime, a negative relationship between precipitation and aerosol loading is observed. However, this does not imply that increased dust suppresses precipitation. Instead, a larger dust burden may augment rain production efficiency through the

alteration of high cloud microphysical processes. Notably, the negative susceptibility of precipitation to dust AOD is predominantly distributed in the southern part of the TP and becomes larger as meteorological conditions strengthen, as shown in Figures S5c-S5e in Supporting Information S1. One may also note that the Ri associated with this regime can be significantly amplified by the addition of more dust, as demonstrated in Figure 2b. Furthermore, the CF exhibits a negative response to dust loading when the PC1 value exceeds approximately 0.8, as shown in Figure 3d, and the meteorological field endorses the formation of intense precipitation in this regime as well.

Consequently, the negative susceptibility of precipitation to AOD can be attributed to the efficient scavenging of dust by the intense rainfall at the top layers of the PC1-IWP bins. This implies that the addition of more dust may maintain or even stimulate stronger precipitation rather than suppress it, subsequently decreasing CF, referred to as the cloud lifetime effect. Thus, dust-induced CF changes depend on a balance between enhanced ice-phased precipitation and modified wet scavenging, which are largely influenced by meteorology. Under moderate meteorology ($-0.3 <$ PC1 < 0.3) with large IWP (IWP > 350 g m^{-2}), CF responses to increased dust aerosols may vary, depending on the equilibrium between dust-induced ice particle promotion and altered particle evaporation/sedimentation rates initiating precipitation. Ultimately, these changes in precipitation, CF, and high cloud microphysical properties determine the net radiative effect of high clouds.

We further derived the dust-mediated high cloud radiative effects in each temporal and spatial grid points (averaged in each PC1/IWP bins) for different aerosol concentration as given in Figure 4. To ensure the robustness of our findings, we conducted a bootstrap test on these results with a significance threshold of 0.99. The majority of the data points passed this statistical test, lending considerable credibility to our observations and subsequent interpretations. The nine subplots organized in ascending AOD order show a notable decreasing trend of cloud radiative forcing when IWP < 200 g m^{-2}, but an increase corresponding to high IWP (IWP > 400 g m^{-2}), as AOD increases from 0.06 to approximately 0.14. This observation substantiates the findings that dust aerosols at lower concentrations can enhance ice particle formation, facilitate precipitation under low IWP, and increase HCF under high IWP. As AOD continues to rise from 0.14 to its maximum value, the net cloud radiative forcing displays a significant decline across IWP levels. This intriguing phenomenon is conceivably attributable to the cumulative effects of intensified precipitation activities within high AOD contexts.

4. Discussion

By utilizing over a decade of reanalysis data alongside multiple satellite observations, we established a leading principal meteorology pattern that exhibits a strong correlation with high-cloud fraction. Combining this pattern with IWP, we isolated the meteorological effects on high clouds and provided robust long-term statistical evidence of the dust aerosol effects on high cloud properties, precipitation, and radiative budget. Our findings show that dust particles facilitate the nucleation process and promotes ice crystals formation under favorable meteorological conditions, subsequently accelerates precipitation by enhancing the aggregation process to produce larger ice particles and accelerating the sedimentation process. Under unfavorable meteorological conditions, particularly with excessive dust aerosols relative to IWP, increasing dust loading will decrease ice particle size, but still can enhance precipitation at the high cloud dissipation stage. These findings implicate that dust aerosols can catalyze high cloud lifecycle, diminish cloud fraction, and ultimately modify high cloud radiative effect.

Although this study focuses on the TP, the implications are far-reaching since dust can have intercontinental transport and profound impacts on global climate system. As the climate continues to warm, the increased loading of dust aerosols resulting from the changes in desertification, land use and atmospheric circulation can significantly influence the lifecycle of high clouds. This feedback increases the occurrence frequency of extreme weather events due to enhanced precipitation on weather scale, which poses a great challenge on water availability, agricultural productivity, and flood risk management. While on climate scale, the increased presence of dust aerosols may reduce high clouds lifetime, thereby potentially mitigate the climate warming that is meaningful for future climate adaptation strategies. By implementing our findings, climate models could more realistically represent the complex feedbacks and radiative effects of dust-high cloud interactions: (a) implementing different cloud simulation schemes explicitly for favorable and unfavorable conditions, adjusting the ice crystal size distribution and number concentration based on both dust loading and atmospheric conditions; (b) updating wet scavenging and cloud lifetime effect algorithms to better capture the intricate interplay between dust loading,
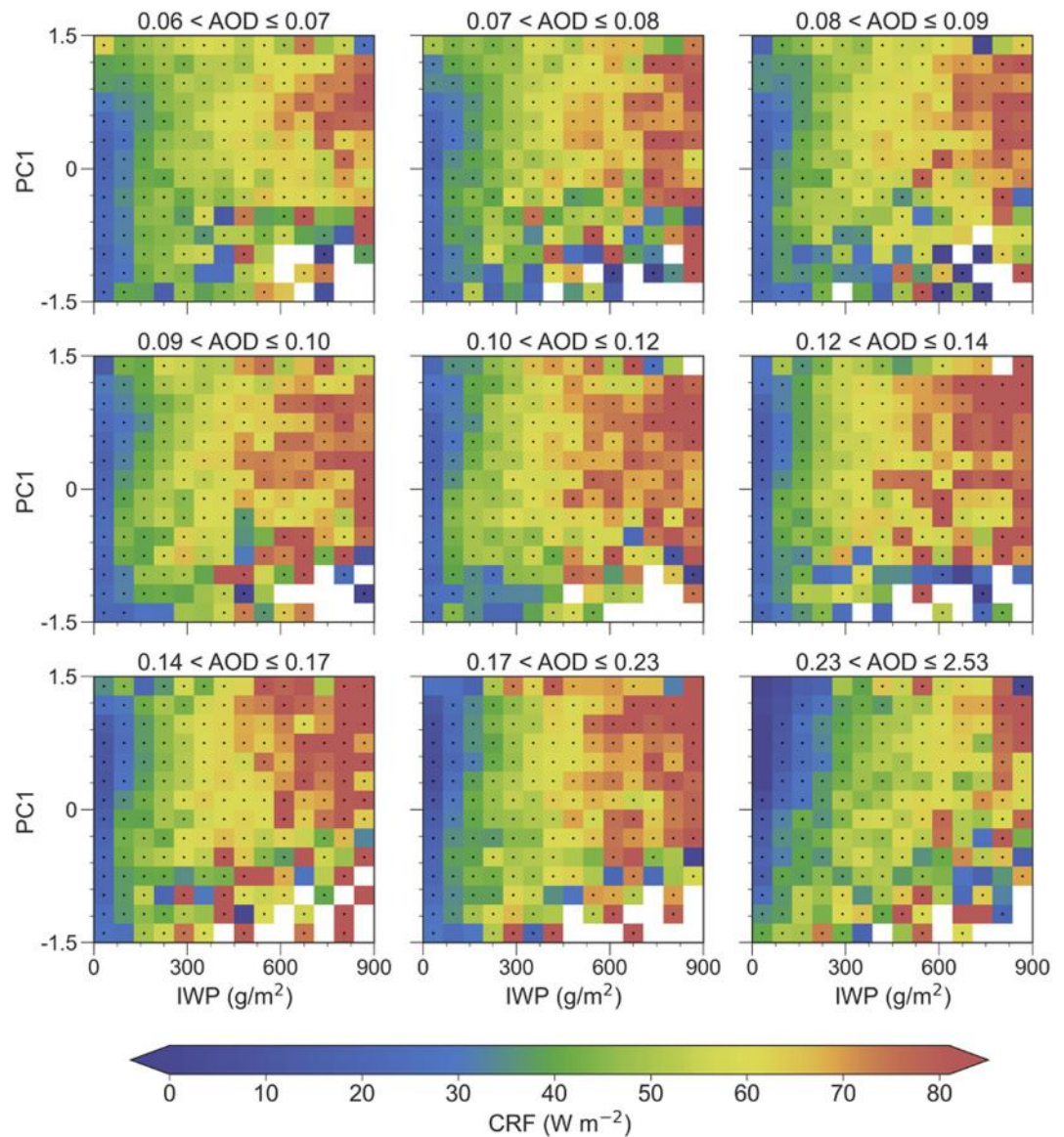
Figure 4. Variation of high cloud radiative forcing with different dust aerosol optical thicknesses under the constraints of the PC1 and the IWP (Black dot indicate that the grid point pass 99% significant test).

precipitation efficiency, and cloud fraction; (c) modifying the fall speed and mass-size relationships of ice crystals based on dust concentrations to more accurately predict the vertical distribution of high clouds.

These findings emphasize the importance of incorporating accurate representations of dust aerosols, their interactions with high clouds and the accelerated sedimentation of ice particles due to dust in numerical models. Such processes are essential to better understand dust effects on high cloud microphysical processes and accurately predict vertical distribution of high cloud and the precipitation, contributing to a more comprehensive understanding of aerosol-cloud interactions and their effects on our weather and climate changes.

Data Availability Statement

The MISR Class 3 aerosol product is available via NASA/LARC/SD/ASDC (2008). The MERRA2 reanalysis data is available by Global Modeling and Assimilation Office (2015). The CERES SYN1deg-Ed4.1 A dataset is

accessible through NASA/LARC/SD/ASDC (2017). The ERA5 reanalysis data can be accessed through Hersbach et al. (2023). The GPM 3IMERG product is available on Huffman et al. (2023).

References

Andreae, M. O., & Rosenfeld, D. (2008). Aerosol–cloud–precipitation interactions. Part 1. The nature and sources of cloud-active aerosols. *Earth-Science Reviews*, *89*(1–2), 13–41. https://doi.org/10.1016/j.earscirev.2008.03.001

Ault, A. P., Williams, C. R., White, A. B., Neiman, P. J., Creamean, J. M., Gaston, C. J., et al. (2011). Detection of asian dust in California orographic precipitation. *Journal of Geophysical Research*, *116*(D16), D16205. https://doi.org/10.1029/2010JD015351

Boose, Y., Baloh, P., Plötze, M., Ofner, J., Grothe, H., Sierau, B., et al. (2019). Heterogeneous ice nucleation on dust particles sourced from nine deserts worldwide – Part 2: Deposition nucleation and condensation freezing. *Atmospheric Chemistry and Physics*, *19*(2), 1059–1076. https://doi.org/10.5194/acp-19-1059-2019

Boose, Y., Welti, A., Atkinson, J., Ramelli, F., Danielczok, A., Bingemer, H. G., et al. (2016). Heterogeneous ice nucleation on dust particles sourced from nine deserts worldwide – Part 1: Immersion freezing. *Atmospheric Chemistry and Physics*, *16*(23), 15075–15095. https://doi.org/10.5194/acp-16-15075-2016

Chen, Y., Chen, S., Zhou, J., Zhao, D., Bi, H., Zhang, Y., et al. (2023). A super dust storm enhanced by radiative feedback. *Npj Climate and Atmospheric Science*, *6*(1), 90. https://doi.org/10.1038/s41612-023-00418-y

Creamean, J. M., Suski, K. J., Rosenfeld, D., Cazorla, A., DeMott, P. J., Sullivan, R. C., et al. (2013). Dust and biological aerosols from the sahara and asia influence precipitation in the western U.S. *Science*, *339*(6127), 1572–1578. https://doi.org/10.1126/science.1227279

Cziczo, D. J., Froyd, K. D., Hoose, C., Jensen, E. J., Diao, M., Zondlo, M. A., et al. (2013). Clarifying the dominant sources and mechanisms of cirrus cloud formation. *Science*, *340*(6138), 1320–1324. https://doi.org/10.1126/science.1234145

Evan, A. T., Flamant, C., Gaetani, M., & Guichard, F. (2016). The past, present and future of african dust. *Nature*, *531*(7595), 493–495. https://doi.org/10.1038/nature17149

Fan, J., Wang, Y., Rosenfeld, D., & Liu, X. (2016). Review of aerosol–cloud interactions: Mechanisms, significance, and challenges. *Journal of the Atmospheric Sciences*, *73*(11), 4221–4252. https://doi.org/10.1175/JAS-D-16-0037.1

Froyd, K. D., Yu, P., Schill, G. P., Brock, C. A., Kupc, A., Williamson, C. J., et al. (2022). Dominant role of mineral dust in cirrus cloud formation revealed by global-scale measurements. *Nature Geoscience*, *15*(3), 177–183. https://doi.org/10.1038/s41561-022-00901-w

Gasparini, B., Meyer, A., Neubauer, D., Münch, S., & Lohmann, U. (2018). Cirrus cloud properties as seen by the *CALIPSO* satellite and ECHAM-HAM global climate model. *Journal of Climate*, *31*(5), 1983–2003. https://doi.org/10.1175/JCLI-D-16-0608.1

Ge, J. M., Huang, J. P., Xu, C. P., Qi, Y. L., & Liu, H. Y. (2014). Characteristics of taklimakan dust emission and distribution: A satellite and reanalysis field perspective: Taklimakan dust characteristics. *Journal of Geophysical Research: Atmospheres*, *119*(20), 11772–11783. https://doi.org/10.1002/2014JD022280

Global Modeling and Assimilation Office (GMAO). (2015). MERRA-2 tavg1_2d_lnd_Nx: 2d,1-Hourly,Time-Averaged,Single-Level,Assimilation,Land surface diagnostics V5.12.4, greenbelt, MD, USA. https://doi.org/10.5067/RKPHT8KC1Y1T.[Dataset]. *Goddard Earth Sciences Data and Information Services Center (GES DISC)*

Hersbach, H., Bell, B., Berrisford, P., Biavati, G., Horányi, A., Muñoz Sabater, J., et al. (2023). ERA5 hourly data on pressure levels from 1940 to present. *Copernicus Climate Change Service (C3S) Climate Data Store (CDS)*. https://doi.org/10.24381/cds.bd0915c6

Hoose, C., & Möhler, O. (2012). Heterogeneous ice nucleation on atmospheric aerosols: A review of results from laboratory experiments. *Atmospheric Chemistry and Physics*, *12*(20), 9817–9854. https://doi.org/10.5194/acp-12-9817-2012

Hu, Z., Huang, J., Zhao, C., Jin, Q., Ma, Y., & Yang, B. (2020). Modeling dust sources, transport, and radiative effects at different altitudes over the Tibetan plateau. *Atmospheric Chemistry and Physics*, *20*(3), 1507–1529. https://doi.org/10.5194/acp-20-1507-2020

Huang, C.-C., Chen, S.-H., Lin, Y.-C., Earl, K., Matsui, T., Lee, H.-H., et al. (2019). Impacts of dust–radiation versus dust–cloud interactions on the development of a modeled mesoscale convective system over north africa. *Monthly Weather Review*, *147*(9), 3301–3326. https://doi.org/10.1175/MWR-D-18-0459.1

Huang, J., Minnis, P., Lin, B., Wang, T., Yi, Y., Hu, Y., et al. (2006). Possible influences of asian dust aerosols on cloud properties and radiative forcing observed from MODIS and CERES. *Geophysical Research Letters*, *33*(6), 2005GL024724. https://doi.org/10.1029/2005GL024724

Huang, J., Wang, T., Wang, W., Li, Z., & Yan, H. (2014). Climate effects of dust aerosols over east asian arid and semiarid regions. *Journal of Geophysical Research: Atmospheres*, *119*(19), 11398–11416. https://doi.org/10.1002/2014JD021796

Huang, J., Zhou, X., Wu, G., Xu, X., Zhao, Q., Liu, Y., et al. (2023). Global climate impacts of land-surface and atmospheric processes over the Tibetan plateau. *Reviews of Geophysics*, *61*(3), e2022RG000771. https://doi.org/10.1029/2022RG000771

Huffman, G. J., Stocker, E. F., Bolvin, D. T., Nelkin, E. J., & Tan, J. (2023). *GPM IMERG final precipitation L3 half hourly 0.1 degree x 0.1 degree V07, greenbelt, MD*. Goddard Earth Sciences Data and Information Services Center (GES DISC). https://doi.org/10.5067/GPM/IMERG/3B-HH/07

Kok, J. F., Storelvmo, T., Karydis, V. A., Adebiyi, A. A., Mahowald, N. M., Evan, A. T., et al. (2023). Mineral dust aerosol impacts on global climate and climate change. *Nature Reviews Earth and Environment*, *4*(2), 71–86. https://doi.org/10.1038/s43017-022-00379-5

Kuebbeler, M., Lohmann, U., Hendricks, J., & Kärcher, B. (2014). Dust ice nuclei effects on cirrus clouds. *Atmospheric Chemistry and Physics*, *14*(6), 3027–3046. https://doi.org/10.5194/acp-14-3027-2014

Liou, K.-N. (1986). Influence of cirrus clouds on weather and climate processes: A global perspective. *Monthly Weather Review*, *114*(6), 1167–1199. https://doi.org/10.1175/1520-0493(1986)114<1167:IOCCOW>2.0.CO;2

Liu, S., Xing, J., Sahu, S. K., Liu, X., Liu, S., Jiang, Y., et al. (2021). Wind-blown dust and its impacts on particulate matter pollution in northern China: Current and future scenarios. *Environmental Research Letters*, *16*(11), 114041. https://doi.org/10.1088/1748-9326/ac31ec

Lohmann, U., & Gasparini, B. (2017). A cirrus cloud climate dial? *Science*, *357*(6348), 248–249. https://doi.org/10.1126/science.aan3325

Ma, P.-L., Rasch, P. J., Chepfer, H., Winker, D. M., & Ghan, S. J. (2018). Observational constraint on cloud susceptibility weakened by aerosol retrieval limitations. *Nature Communications*, *9*(1), 2640. https://doi.org/10.1038/s41467-018-05028-4

NASA/LARC/SD/ASDC. (2008). MISR Level 3 Component Global Aerosol product in netCDF format covering a day V004. [Dataset]. https://doi.org/10.5067/Terra/MISR/MIL3DAEN_L3.004.NASA Langley Atmospheric Science Data Center DAAC

NASA/LARC/SD/ASDC. (2017). CERES and GEO-enhanced TOA, within-atmosphere and surface fluxes, clouds and aerosols 1-hourly terra-aqua Edition4A. [Dataset]. Retrieved from https://doi.org/10.5067/TERRA+AQUA/CERES/SYN1DEG-1HOUR_L3.004A. NASA Langley Atmospheric Science Data Center DAAC

Patel, P. N., Gautam, R., Michibata, T., & Gadhavi, H. (2019). Strengthened Indian summer monsoon precipitation susceptibility linked to dust-induced ice cloud modification. *Geophysical Research Letters*, *46*(14), 8431–8441. https://doi.org/10.1029/2018GL081634

Rajeevan, M., & Srinivasan, J. (2000). Net cloud radiative forcing at the top of the atmosphere in the asian monsoon region. *Journal of Climate*, *13*(3), 650–657. https://doi.org/10.1175/1520-0442(2000)013<0650:NCRFAT>2.0.CO;2

Rosenfeld, D., Lohmann, U., Raga, G. B., O'Dowd, C. D., Kulmala, M., Fuzzi, S., et al. (2008). Flood or drought: How do aerosols affect precipitation? *Science*, *321*(5894), 1309–1313. https://doi.org/10.1126/science.1160606

Rosenfeld, D., Rudich, Y., & Lahav, R. (2001). Desert dust suppressing precipitation: A possible desertification feedback loop. *Proceedings of the National Academy of Sciences*, *98*(11), 5975–5980. https://doi.org/10.1073/pnas.101122798

Rosenfeld, D., Zhu, Y., Wang, M., Zheng, Y., Goren, T., & Yu, S. (2019). Aerosol-driven droplet concentrations dominate coverage and water of oceanic low-level clouds. *Science*, *363*(6427), eaav0566. https://doi.org/10.1126/science.aav0566

Seinfeld, J. H., Bretherton, C., Carslaw, K. S., Coe, H., DeMott, P. J., Dunlea, E. J., et al. (2016). Improving our fundamental understanding of the role of aerosol−cloud interactions in the climate system. *Proceedings of the National Academy of Sciences*, *113*(21), 5781–5790. https://doi.org/10.1073/pnas.1514043113

Sorooshian, A., Anderson, B., Bauer, S. E., Braun, R. A., Cairns, B., Crosbie, E., et al. (2019). Aerosol–cloud–meteorology interaction airborne field investigations: Using lessons learned from the U.S. west coast in the design of ACTIVATE off the U.S. east coast. *Bulletin of the American Meteorological Society*, *100*(8), 1511–1528. https://doi.org/10.1175/BAMS-D-18-0100.1

Stevens, B., & Feingold, G. (2009). Untangling aerosol effects on clouds and precipitation in a buffered system. *Nature*, *461*(7264), 607–613. https://doi.org/10.1038/nature08281

Uno, I., Eguchi, K., Yumimoto, K., Takemura, T., Shimizu, A., Uematsu, M., et al. (2009). Asian dust transported one full circuit around the globe. *Nature Geoscience*, *2*(8), 557–560. https://doi.org/10.1038/ngeo583

Wu, G., Duan, A., Liu, Y., Mao, J., Ren, R., Bao, Q., et al. (2015). Tibetan plateau climate dynamics: Recent research progress and outlook. *National Science Review*, *2*(1), 100–116. https://doi.org/10.1093/nsr/nwu045

Zhao, B., Liou, K.-N., Gu, Y., Jiang, J. H., Li, Q., Fu, R., et al. (2018). Impact of aerosols on ice crystal size. *Atmospheric Chemistry and Physics*, *18*(2), 1065–1078. https://doi.org/10.5194/acp-18-1065-2018

Zhao, B., Wang, Y., Gu, Y., Liou, K.-N., Jiang, J. H., Fan, J., et al. (2019). Ice nucleation by aerosols from anthropogenic pollution. *Nature Geoscience*, *12*(8), 602–607. https://doi.org/10.1038/s41561-019-0389-4